Supplementary Information for "Quantum Simulation of the non-Fermi-Liquid State of Sachdev-Ye-Kitaev Model"

1. Hamiltonian parameters of the generalized SYK model. The Hamiltonian of $(0+1)d$ generalized SYK model with $N = 8$ Majorana fermions is given by

$$H = \frac{J_{ijkl}}{4!}\chi_i\chi_j\chi_k\chi_l + \frac{\mu}{4}C_{ij}C_{kl}\chi_i\chi_j\chi_k\chi_l. \tag{S1}$$

The antisymmetric random tensors of J_{ijkl} and C_{ij} are drawn from the Gaussian distribution: $\overline{J_{ijkl}} = 0, \overline{J_{ijkl}^2} = 3!J_4^2/N^3$ and $\overline{C_{ij}} = 0, \overline{C_{ij}C_{kl}} = 2J^2/N^2(\delta_{ik}\delta_{jl} - \delta_{il}\delta_{jk})$ (here $J = \sqrt{J_4} = 1$), and plotted in Figs. S1(a) and S1(b), respectively. For $N = 8$, there are 70 J_{ijkl}s and 28 C_{ij}s in each sample or a random Hamiltonian. In experiments, we randomly generated $r = 1, 2, \ldots, 8$ different Hamiltonians.

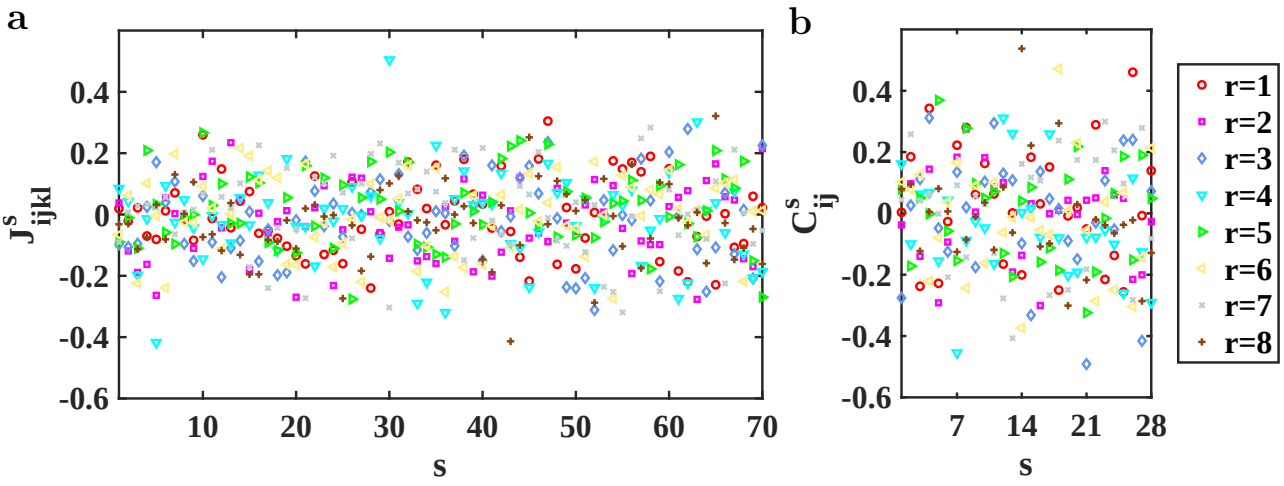

FIG. S1: Antisymmetric random Tensors of J_{ijkl} and C_{ij} in different random Hamiltonians.

Using the Jordan-Wigner transformation, Hamiltonian (S1) can be rewritten as the sum of spin interactions,

$$H = \sum_{s=1}^{70} H_s = \sum_{s=1}^{70} a^s_{ijkl}\sigma^1_{\alpha_i}\sigma^2_{\alpha_j}\sigma^3_{\alpha_k}\sigma^4_{\alpha_l}, \tag{S2}$$

where subscripts $\alpha = \{0, x, y, z\}$ label the corresponding Pauli matrices, and $\sigma_0 = \mathbb{I}$. All subscripts of spin interactions are listed in Table. S1. For example, the first term of $xx00$ in Table. S1 represents the 2-body spin interaction, i.e., $\sigma^1_x\sigma^2_x$. The random coefficients of a^s_{ijkl} for different μ are shown in Fig. S2.

TABLE S1: The subscripts for denoting the spin interactions in Hamiltonian (S2).

$xx00$	$xyxy$	$xyxz$	$xyy0$	$xyz0$	$xzxy$	$xzxz$	$xzy0$	$xzz0$	$x0x0$	$x0yy$	$x0yz$	$x0zy$	$x0zz$
$x00x$	$yxyx$	$yxzx$	$yx0y$	$yx0z$	$yyx0$	$yyyy$	$yyyz$	$yyzy$	$yyzz$	$yy0x$	$yzx0$	$yzyy$	$yzyz$
$yzzy$	$yzzz$	$yz0x$	$y0xy$	$y0xz$	$y0y0$	$y0z0$	$zxyx$	$zxzx$	$zx0y$	$zx0z$	$zyx0$	$zyyy$	$zyyz$
$zyzy$	$zyzz$	$zy0x$	$zzx0$	$zzyy$	$zzyz$	$zzzy$	$zzzz$	$zz0x$	$z0xy$	$z0xz$	$z0y0$	$z0z0$	$0xx0$
$0xyy$	$0xyz$	$0xzy$	$0xzz$	$0x0x$	$0yyx$	$0yzx$	$0y0y$	$0y0z$	$0zyx$	$0zzx$	$0z0y$	$0z0z$	$00xx$

2. Relevant parameters of the nuclear spin system. The physical system used in the experiment consists of four carbon-13 nuclear spins of trans-crotonic acid. Its relevant parameters including chemical shifts, J-couplings and relaxation times are shown in Table. S2.

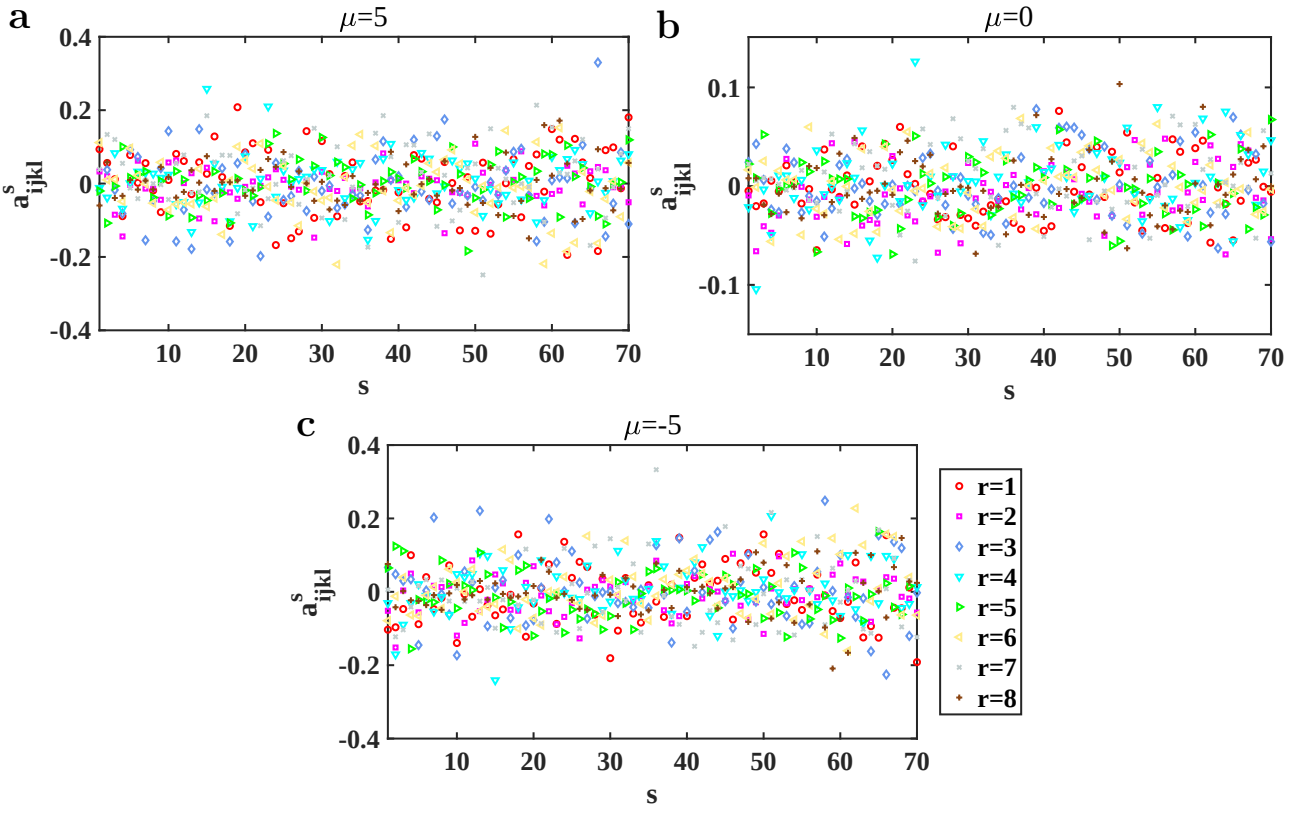

FIG. S2: Random coefficients of a^s_{ijkl} for different μ.

TABLE S2: The Hamiltonianl parameters of trans-crotonic acid. Diagonal and off-diagonal elements represent the chemical shifts and J-coupling constants (in Hz), respectively. The measured spin-lattice relaxation times T_1 (in seconds) and spin-spin relaxation times T_2 (in seconds) are shown in the last two columns.

	$\mathbf{C_1}$	$\mathbf{C_2}$	$\mathbf{C_3}$	$\mathbf{C_4}$	$\boldsymbol{T_1(s)}$	$\boldsymbol{T_2(s)}$
$\mathbf{C_1}$	2989				5.7	1.02
$\mathbf{C_2}$	41.6	25459			5.3	0.92
$\mathbf{C_3}$	1.4	69.7	21592		5.6	0.89
$\mathbf{C_4}$	7.0	1.2	72.2	29341	10.2	0.94

3. Rotation angles for preparing initial states. The initial 'states' that need to be prepared in our experiments are $\rho_i^{\text{Real}} = (\rho_{\text{eq}}^H b + b\rho_{\text{eq}}^H)/2$ and $\rho_i^{\text{Imag}} = -i(\rho_{\text{eq}}^H b - b\rho_{\text{eq}}^H)/2$, where $\rho_{\text{eq}}^H = e^{-\beta H}/\text{Tr}(e^{-\beta H})$. Given a random Hamiltonian and temperature β, the sixteen single-qubit rotations and free evolutions of nature NMR Hamiltonian enable the system to be prepared into the specific states, i.e., their diagonal elements of density matrices equal to the eigenvalues of these initial 'states' . The single-qubit rotation angles for preparing $\rho_i^{\text{Real}}(\beta,\mu)$ and $\rho_i^{\text{Imag}}(\beta,\mu)$ in different random Hamiltonians are shown in Fig. S3. When $\beta = 0$, $\rho_i^{\text{Imag}}(0,\mu) = 0$ for any μ, and is not necessary to be prepared.

4. Details of experimental simulation. The generalized SYK model can be simulated by a fully controllable quantum system, i.e., the four nuclear spins of trans-crotonic acid used in our experiment. As illustrated in Fig. S4, the simulation procedure is stated as follows: After mapping the generalized SYK Hamiltonian (S1) onto a spin model via the Jordan-Wigner transformations, the resulting Hamiltonian (S2) consisting of a sum of 70 local k-body ($k \leq 4$) spin interactions, as listed in Table. S1, can be effectively simulated by evolving the system forward locally over small, discrete time slices, i.e., simulating the local time evolution operators $e^{-iH_1\tau/n}, e^{-iH_2\tau/n}$, and so on, up to $e^{-iH_{70}\tau/n}$, and repeating n times. Here we use the Trotter-Suzuki approximation decomposition of $e^{-iH\tau} \approx (e^{-iH_1\tau/n}\cdots e^{-iH_{70}\tau/n})^n$, which takes place to within some desired accuracy by choosing sufficiently large

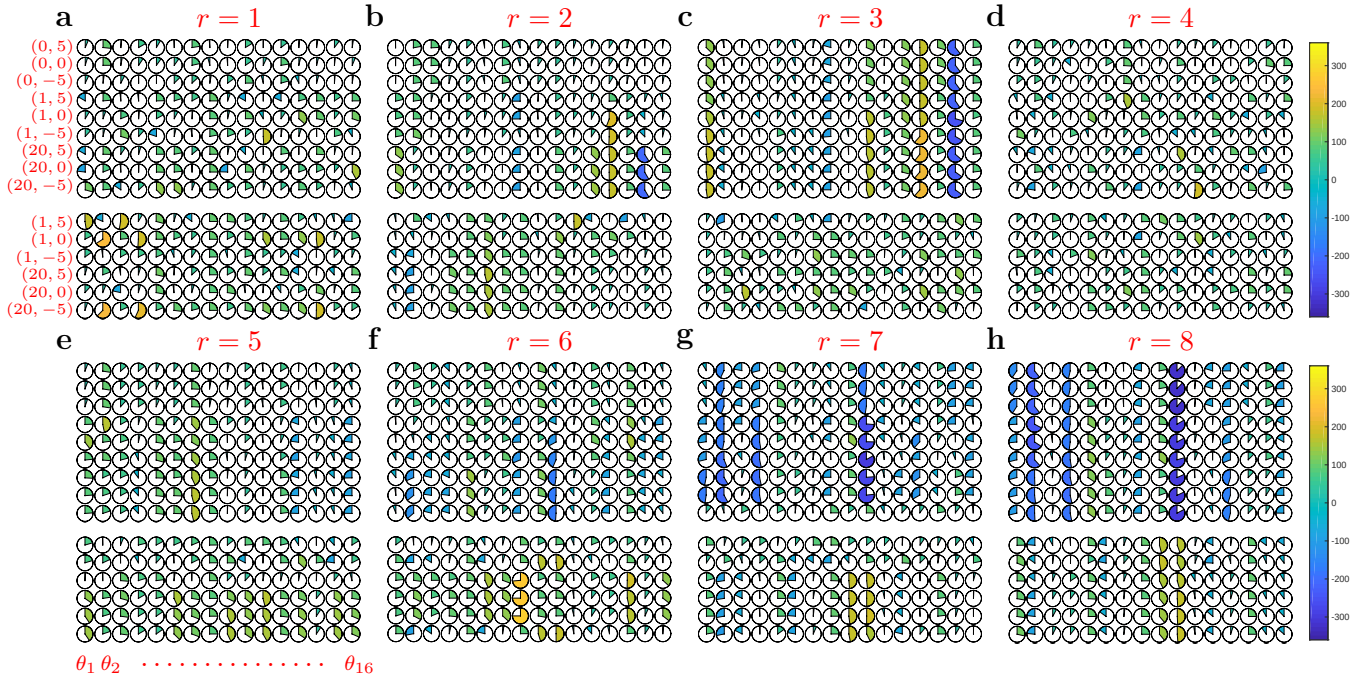

FIG. S3: The single-qubit rotation angles (degree unit) for preparing initial states $\rho_i(\beta,\mu)$ in different random Hamiltonians, where $\beta = 0, 1, 20$ and $\mu = 5, 0, -5$. The top and bottom panels are used to prepare $\rho_i^{\rm Real}(\beta,\mu)$ and $\rho_i^{\rm Imag}(\beta,\mu)$, respectively. Because $\rho_i^{\rm Imag}(0,\mu) = 0$, there is no rotation angle listed here.

n, as shown in Fig. 3a. Now the issue of experimental simulation turns into how to implement the discrete time evolutions of local k-body spin interactions, $e^{-iH_s\tau/n} = e^{-ia^s_{ijkl}\sigma^1_{\alpha_i}\sigma^2_{\alpha_j}\sigma^3_{\alpha_k}\sigma^4_{\alpha_l}\tau/n}$, for $s = 1, \cdots, 70$, by a NMR quantum simulator.

The NMR quantum simulator, relying the coherent control of nuclear spins, would allow resolving the above issue of experimentally simulating many-body spin interactions. Let us first review our NMR system in the main paper. Its internal Hamiltonian is $H_{\rm NMR} = \sum_{i=1}^4 \frac{\omega_i}{2}\sigma_z^i + \sum_{i<j,=1}^4 \frac{\pi J_{ij}}{2}\sigma_z^i\sigma_z^j$, which consists of 1-body interactions and 2-body interactions. The external or control Hamiltonian describing the effect of radio-frequency (RF) pulses is $H_{\rm C} = \sum_{i=1}^4 B_i[\cos(\omega^i_{\rm RF}t + \phi_i)\sigma_x^i + \sin(\omega^i_{\rm RF}t + \phi_i)\sigma_y^i]$. By designing a specific pulse sequence (i.e., choosing the appropriate amplitudes B_i, frequencies $\omega^i_{\rm RF}$, phases ϕ_i and pulse durations τ), each local time evolution operator $e^{-iH_s\tau/n}$ is readily implemented. For example, the pulse sequences in the rotating frame (we set the reference frequency $\omega_{\rm ref} = \omega^j_{\rm RF} = 176.053$ MHz in experiments) for simulating 1-, 2-, 3-, and 4-body interactions are given below:

1. For $e^{-i\pi J_1\tau\sigma_x^1/2}$, $[\theta]_x^1$, where $\theta = \pi J_1\tau$;
2. For $e^{-i\pi J_{12}\tau\sigma_z^1\sigma_z^2/2}$, $\{\frac{\tau}{4}\} \to [\pi]_y^4 \to \{\frac{\tau}{4}\} \to [\pi]_y^3 \to \{\frac{\tau}{4}\} \to [\pi]_y^4 \to \{\frac{\tau}{4}\}$;
3. For $e^{-i\pi J_{123}\tau\sigma_z^1\sigma_z^2\sigma_z^3/2}$, $[\frac{\pi}{2}]_x^2 \to [\pi]_y^2 \to [\frac{1}{2J_{12}}] \to [-\frac{\pi}{2}]_y^2 \to [\frac{J_{123}\tau}{J_{23}}] \to [-\frac{\pi}{2}]_y^2 \to [\frac{1}{2J_{12}}] \to [-\frac{\pi}{2}]_x^2$;
4. For $e^{-i\pi J_{1234}\tau\sigma_z^1\sigma_z^2\sigma_z^3\sigma_z^4/2}$, $[\frac{\pi}{2}]_x^2 \to [\pi]_y^2 \to [\frac{1}{2J_{12}}] \to [-\frac{\pi}{2}]_y^2 \to [\frac{\pi}{2}]_x^3 \to [\pi]_y^3 \to [\frac{1}{2J_{23}}] \to [-\frac{\pi}{2}]_y^3 \to [\frac{J_{1234}\tau}{J_{34}}] \to [-\frac{\pi}{2}]_y^3 \to [\frac{1}{2J_{23}}] \to [-\frac{\pi}{2}]_x^3 \to [-\frac{\pi}{2}]_y^2 \to [\frac{1}{2J_{12}}] \to [-\frac{\pi}{2}]_x^2$.

Here we denote the above symbols as $[\theta]_\alpha^j = e^{-i\theta\sigma_\alpha^j}, [\tau_{jk}] = e^{-i\pi J_{jk}\tau\sigma_z^j\sigma_z^k/2}$, and $\{\tau\} = e^{-iH_{\rm NMR}\tau}$, for simplicity. It could be found that the first case of 1-body interaction can be created by a single pulse of rotation, several refocusing-π pulses can realize the specific 2-body interaction, and the cases of 3-,4-body interactions can be implemented by the combination of 1- and 2-body interactions.

For our case of $(e^{-iH_1\tau/n}\cdots e^{-iH_{70}\tau/n})^n = \prod_{j=1}^M e^{-i[H_{\rm NMR}+H_{\rm C}(B_j,\phi_j)]\tau/M}$, we employ the gradient ascent pulse engineering (GRAPE) algorithm [1] to find its control fields, i.e., the amplitudes B_js and phases ϕ_js. The resulting profiles of a shaped pulse with the slices of $M = 4000$ and duration of 100 ms are shown in Fig. S5. To improve the

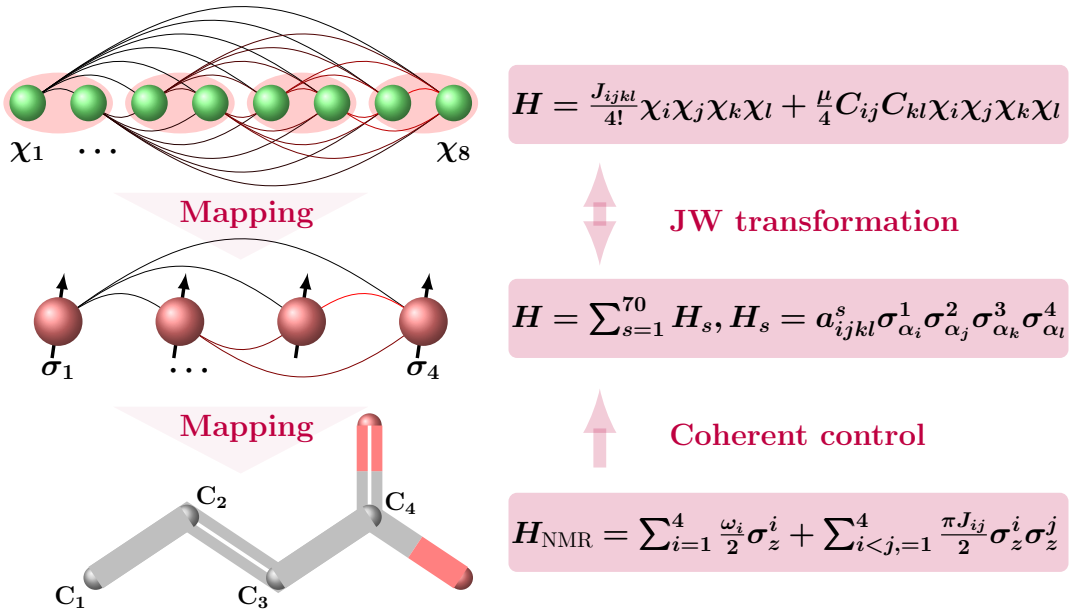

FIG. S4: Scheme for experimentally simulating the generalized SYK model. The generalized SYK model is firstly mapped onto a spin model via the Jordan-Wigner (JW) transformation, and then we simulate this spin model by the means of coherent control acting on the physical system of nuclear spins in trans-crotonic acid. The procedure can also be clear from the following change of time evolution operators: $e^{-iH\tau} \leftrightarrow e^{-i\sum_{s=1}^{70} H_s\tau} \approx \left(\prod_{s=1}^{70} e^{-iH_s\tau/n}\right)^n \leftarrow \prod_{j=1}^{M} e^{-i(H_{\mathrm{NMR}}+H_{\mathrm{C}}(B_j,\phi_j)\tau/M}$. The task in coherent control is to design a pulse sequence for finding the amplitudes B_js and phases ϕ_js of radio-frequency fields.

control performance in simulating the evolution of generalized SYK model, the shaped pulse was designed to have over 99% numerical fidelity in present of 5% the inhomogeneity of radio-frequency fields.

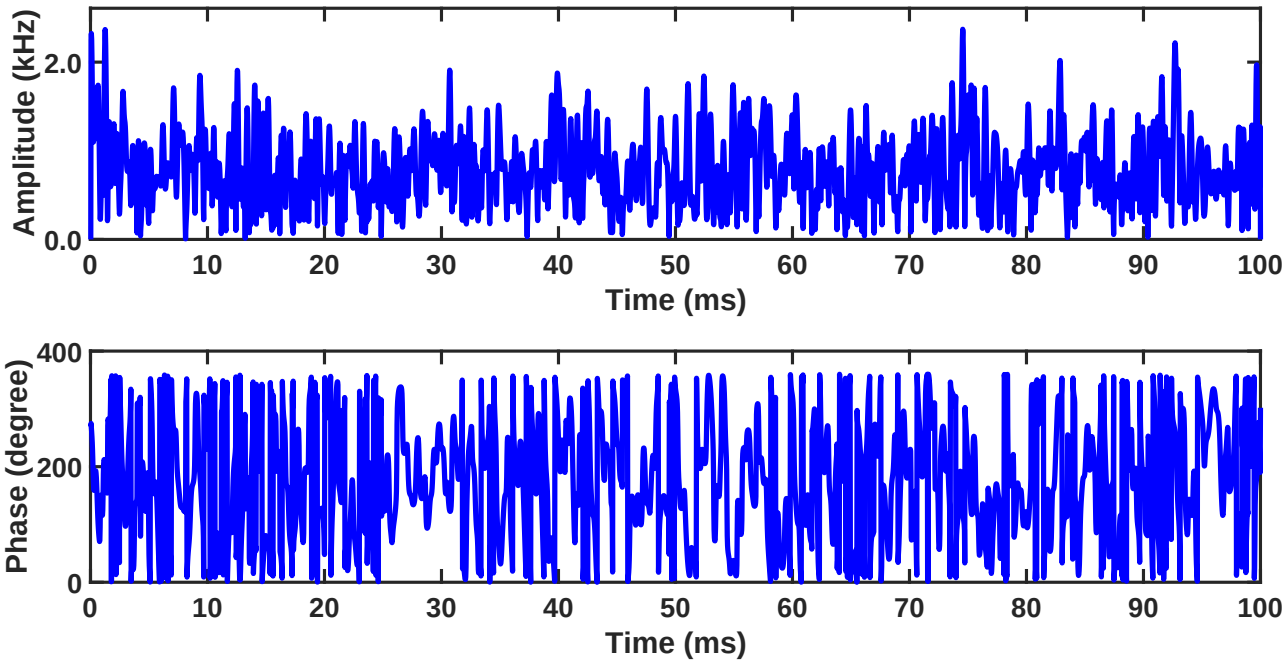

FIG. S5: The shaped pulse for implementing the evolution of generalized SYK model. Its amplitudes and phases are shown in the top and in the bottom, respectively. The pulse has 4000 slices, and the total duration is 100 ms.

5. Experimental results for different random samples. The main experimental results in body paper were obtained by averaging over eight random samples. The boson correlation functions for $r = 1, 2, \ldots, 8$ random samples are shown in Figs. S6(a) $\sim$ S6(h), respectively.

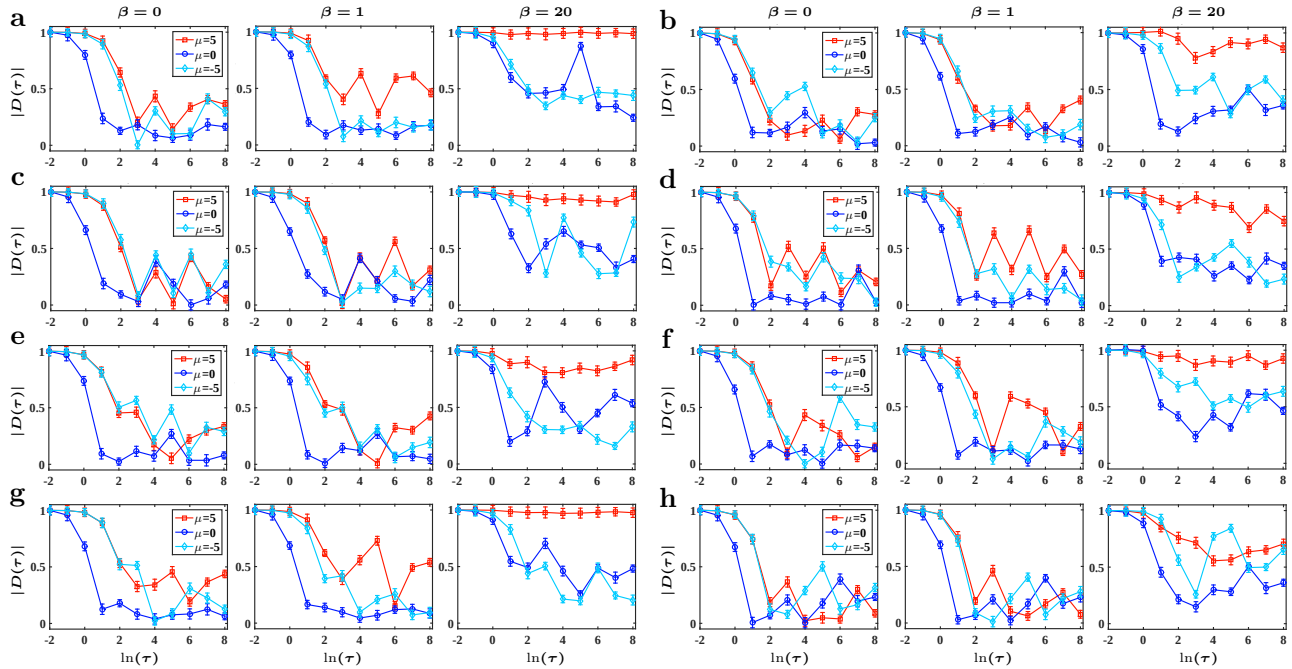

FIG. S6: The resulting boson correlation functions for $r = 1, 2, \ldots, 8$ random samples. The error bars are calculated from the fitting procedure.

6. Scaling behavior. It is technically challenging to study a larger system experimentally, thus we resort to numerical simulation to check the scaling behavior. Figure S7 shows the system size dependence of avg$|D(\infty)|$ for $N = 6, 8, \cdots, 18$. In the non-Fermi liquid phase ($\mu \leq 0$), the saturate value of boson correlation decays towards zero with system size. In the symmetry breaking phase ($\mu > 0$), the saturate value scales towards a finite value in the thermodynamic limit.

[1] Khaneja, N., Reiss, T., Kehlet, C., Schulte-Herbrüggen, T. & Glaser, S. J. Optimal control of coupled spin dynamics: design of nmr pulse sequences by gradient ascent algorithms. *Journal of magnetic resonance* **172**, 296–305 (2005).

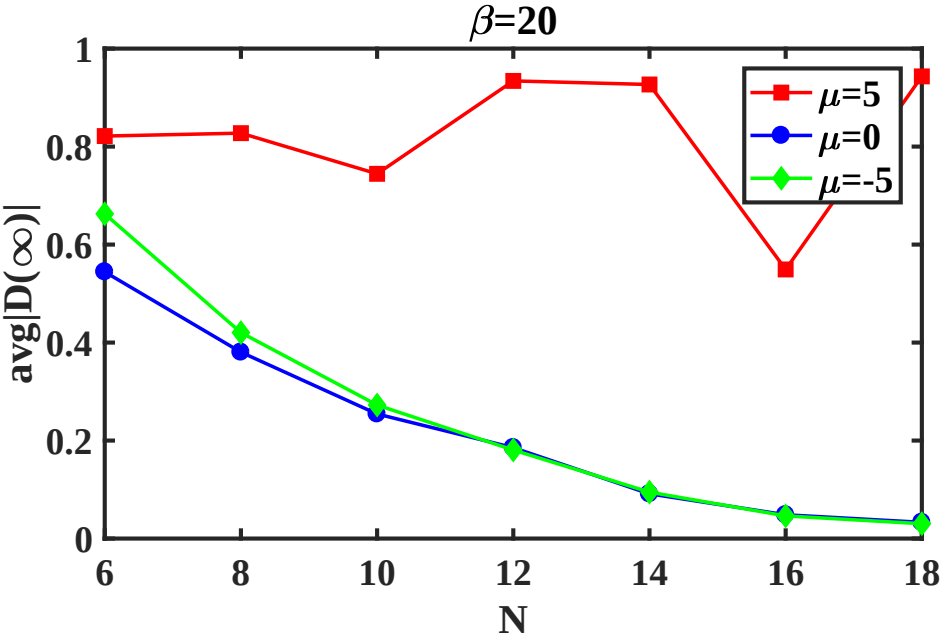

FIG. S7: System size N dependence of avg$|D(\infty)|$ at low temperature of $\beta = 20$. The boson correlations for $\mu \leq 0$ will decay to zero with the grows of system size; While for $\mu > 0$, the boson correlation will saturate to a finite value in thermodynamic limit.